

letters to nature

15. D'Alessandro, E. & McCulloch, P. M. Long-term timing observations of four southern pulsars. *Mon. Not. R. Astron. Soc.* **292**, 879–886 (1997).
16. Mereghetti, S. A spin-down variation in the 6 second X-ray pulsar 1E 1048.1-5937. *Astrophys. J.* **455**, 598–602 (1995).
17. Melatos, A. Bumpy spin-down of anomalous X-ray pulsars: The link with magnetars. *Astrophys. J.* **519**, 177–180 (1999).
18. Alpar, M. A., Anderson, P. W., Pines, D. & Shaham, J. Vortex creep and the internal temperature of neutron stars. I. General theory. *Astrophys. J.* **276**, 325–334 (1984).
19. Roberts, D. H., Lehar, J. & Dreher, J. W. Time series analysis with CLEAN. I. Derivation of a spectrum. *Astron. J.* **93**, 968–989 (1987).
20. Lyne, A. G. & Graham-Smith, F. *Pulsar Astronomy*, 14–22 (Cambridge, Univ. Press, Cambridge, 1998).

Acknowledgements

We thank D. J. Nice for providing the two-standard-profile frequency-domain fitting routine, M. Goss for obtaining the interferometric pulsar position, F. Graham Smith for reading of the manuscript and F. Camilo for discussions. I.H.S. received support from a Natural Sciences and Engineering Research Council of Canada postdoctoral fellowship.

Correspondence and requests for materials should be addressed to A.G.L. (e-mail: agl@jb.man.ac.uk).

Vortex-like excitations and the onset of superconducting phase fluctuation in underdoped $\text{La}_{2-x}\text{Sr}_x\text{CuO}_4$

Z. A. Xu^{*†}, N. P. Ong^{*}, Y. Wang^{*}, T. Kakeshita[‡] & S. Uchida[‡]

^{*} Joseph Henry Laboratories of Physics, Princeton University, Princeton, New Jersey 08544, USA

[‡] School of Frontier Sciences, University of Tokyo, Yayoi 2-11-16, Bunkyo-ku, Tokyo 113-8656, Japan

Two general features of a superconductor, which appear at the critical temperature, are the formation of an energy gap and the expulsion of magnetic flux (the Meissner effect). In underdoped copper oxides, there is strong evidence that an energy gap (the pseudogap¹) opens up at a temperature significantly higher than the critical temperature (by 100–220 K). Certain features of the pseudogap suggest that it is closely related to the gap that appears at the critical temperature (for example, the variation of the gap magnitudes around the Fermi surface and their maximum amplitudes are very similar^{2,3}). However, the Meissner effect is absent in the pseudogap state. The nature of the pseudogap state, and its relation (if any) to the superconducting state are central issues in understanding copper oxide superconductivity. Recent evidence suggests that, in the underdoped regime, the Meissner state is destroyed above the critical temperature by strong phase fluctuations^{4–7} (as opposed to a vanishing of the superfluid density). Here we report evidence for vortices (or vortex-like excitations) in $\text{La}_{2-x}\text{Sr}_x\text{CuO}_4$ at temperatures significantly above the critical temperature. A thermal gradient is applied to the sample in a magnetic field. Vortices are detected by the large transverse electric field produced as they diffuse down the gradient (the Nernst effect). We find that the Nernst signal is anomalously enhanced at temperatures as high as 150 K.

In conventional superconductors, fluctuations in the phase $\theta(r)$ of the superconducting wavefunction $\psi \exp[i\theta(r)]$ incur a sizeable cost in energy (the phase stiffness energy is large). Hence $\theta(r)$ is uniform in the absence of field and currents. In the underdoped

copper oxides, however, the small superfluid density n_s implies a small phase stiffness energy⁴. The Meissner state is readily destroyed by strong phase fluctuations. This suggests that rapidly diffusing vortices, which are highly effective in destroying phase coherence, may help to limit the critical temperature T_c . In a recent experiment, Corson *et al.*⁷ measured the complex conductivity in underdoped $\text{Bi}_2\text{Sr}_2\text{CaCu}_2\text{O}_{8+\delta}$ (BSCCO) at terahertz frequencies, and deduced a Kosterlitz–Thouless transition⁸ at T_c , with a fluctuating regime that extends about 25 K above T_c .

To detect directly the presence of vortices above T_c , we have adopted a different approach. By using a strictly d.c. probe that selectively senses vortex motion, we may detect excitations that are long-lived. An applied thermal gradient ($-\nabla T$) causes vortices to diffuse with a velocity \mathbf{v} (\mathbf{v} may be tilted relative to $-\nabla T$). The distinguishing feature of moving vortices is the Josephson electric field given by $\mathbf{E} = \mathbf{B} \times \mathbf{v}$, which reflects phase slippage caused by moving vortices. The y -component of the \mathbf{E} -field leads to a very large Nernst effect. With $-\nabla T \parallel x$, the Nernst coefficient is defined as

$$\nu = E_y / (B |\nabla T|) \quad (1)$$

with the induction field $\mathbf{B} \parallel z$. (Previous Nernst experiments in the copper oxides were restricted to optimally doped samples^{9–11}.) In our experiment, we measured ν versus T in five crystals of $\text{La}_{2-x}\text{Sr}_x\text{CuO}_4$ (LSCO; samples 1–5), with $0.05 < x < 0.17$, and in a crystal of Nd-doped $\text{La}_{2-y-x}\text{Nd}_y\text{Sr}_x\text{CuO}_4$ (sample N).

Figure 1 displays traces of the Nernst signal E_y versus the applied field H in sample 3 ($x = 0.10$) at temperatures between 12 and 35 K (Fig. 1a) and above 35 K (Fig. 1b). At 12 and 15 K, the behaviour

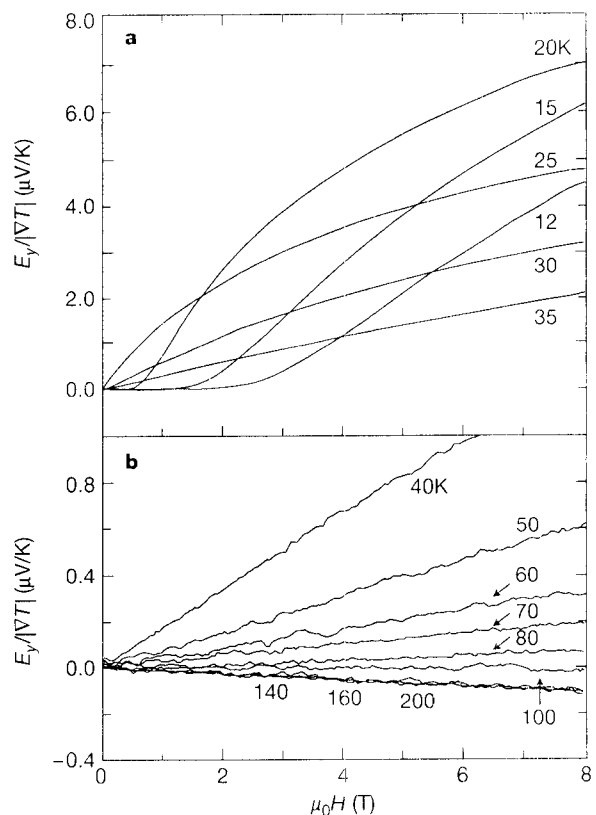


Figure 1 Nernst signals. **a**, The Nernst signal E_y (normalized to unit gradient) versus $H \parallel c$ in $\text{La}_{2-x}\text{Sr}_x\text{CuO}_4$ (sample 3, $x = 0.10$) at temperatures 12–35 K. **b**, The Nernst signal from 40 to 200 K. Above 20 K, the applied gradient is 5 K cm^{-1} , while below 20 K, it is half as large. When vortex pinning is large ($T < 25 \text{ K}$), E_y is zero over a range of $H < H_m$. Above 140 K, the curves tend asymptotically to a straight line of negative slope.

[†] Present address: Department of Physics, Zhejiang University, Hangzhou 310027, China.

of E_y versus H resembles the flux-flow resistivity. When H exceeds a T -dependent field scale H_m , the onset of vortex motion produces a large Nernst signal that increases rapidly with H in accordance with $\mathbf{E} = \mathbf{B} \times \mathbf{v}$. The surprising feature is that the Nernst signal is a sizeable fraction of the low- T values above $T_c = 28$ K (see curves at 30 and 35 K). At higher T (Fig. 1b), the signal decreases, gradually approaching a straight line of negative slope, which we identify with the background signal ν_n from the holes. Similar traces are obtained in all samples studied. The Nernst coefficient ν , calculated from the initial slope of E_y versus H , is shown for samples 1–5 in log–log scale in Fig. 2 (with the background ν_n subtracted). In each sample, the maximum value of ν ($\sim 2 \mu\text{V}/\text{KT}$) is similar to that in $\text{YBa}_2\text{Cu}_3\text{O}_7$ (YBCO)¹⁰. With increasing T , ν falls by two decades from its peak value to the normal-state value ν_n . Comparing across samples, we noticed a systematic trend of the rate of decrease of ν above T_c (arrows). As x decreases from 0.17 to 0.05, ν falls less and less steeply. To display this trend more clearly, we show in expanded (linear) scale the behaviour of ν at high T (Fig. 3a). The arrows indicate the onset temperature T_{onset} at which we resolve the anomalous signal from the background ν_n (broken horizontal lines). As x decreases from 0.17 to 0.05, the interval between T_c and T_{onset} in each sample systematically expands. In the most underdoped samples (1 and 2), the Nernst signal is anomalously enhanced up to about 150 K. The enhanced signal presents intriguing evidence for vortices or vortex-like excitations that persist to elevated temperatures.

For comparison, we discuss the ‘weak’ Nernst background originating from the action of the Lorentz force on the diffusing holes (that is, in the absence of vortices). In an \mathbf{E} -field and a gradient $-\nabla T$, the current density is comprised of two terms: $\mathbf{J} = \alpha(-\nabla T) + \sigma\mathbf{E}$, where σ is the two-dimensional electrical conductivity tensor, and α the two-dimensional conductivity tensor. In a magnetic field $\mathbf{B} \parallel \mathbf{z}$, the two terms produce Hall currents

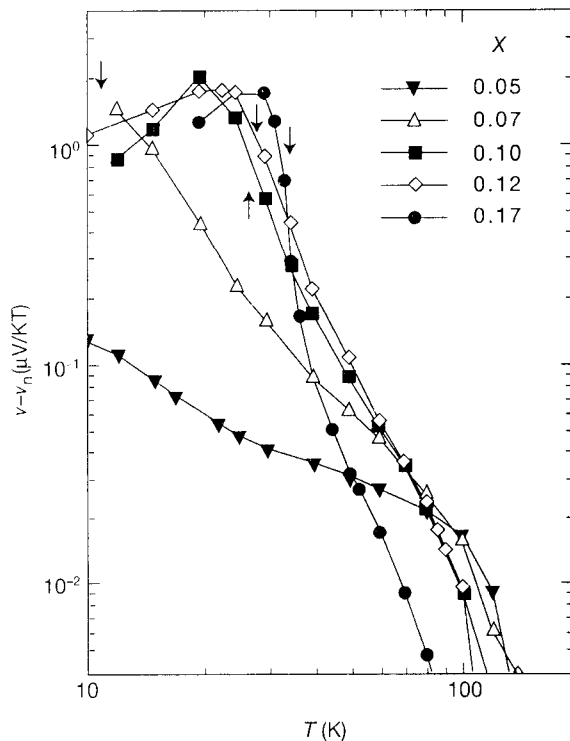


Figure 2 Log–log plot of the anomalous part of the Nernst coefficient. $\nu - \nu_n$ versus T in LSCO is plotted for samples 1–5, with $x(T_c) = 0.05$ (<4 K), 0.07 (11 K), 0.10 (27.5 K), 0.12 (29 K) and 0.17 (35.4 K), respectively. As x decreases, the rate of decrease of ν above T_c (arrows) decreases, while the onset temperature increases.

along y of opposite signs which result in a strongly reduced Nernst coefficient¹² (see legend of Fig. 3):

$$E_y/(\mathbf{B}|\nabla T) = [(\alpha_{xy}/\sigma) - (\alpha/\sigma)(\sigma_{xy}/\sigma)]/B \quad (2)$$

where σ and α are the diagonal elements of σ and α , respectively. The second term may be re-cast as $-S \tan\theta_H/B$, with S the thermopower and $\tan\theta_H$ the Hall angle. We verify that the cancellation between the two terms is nearly complete in LSCO. In each sample, we have measured S and σ_{xy} separately in order to calculate $S \tan\theta_H/B$. With decreasing T , $S \tan\theta_H/B$ displays a broad maximum (solid symbols in Fig. 3a). In comparing its value with ν (in sample 2 above 130 K, for example), it is clear that the latter is about 30 times smaller, that

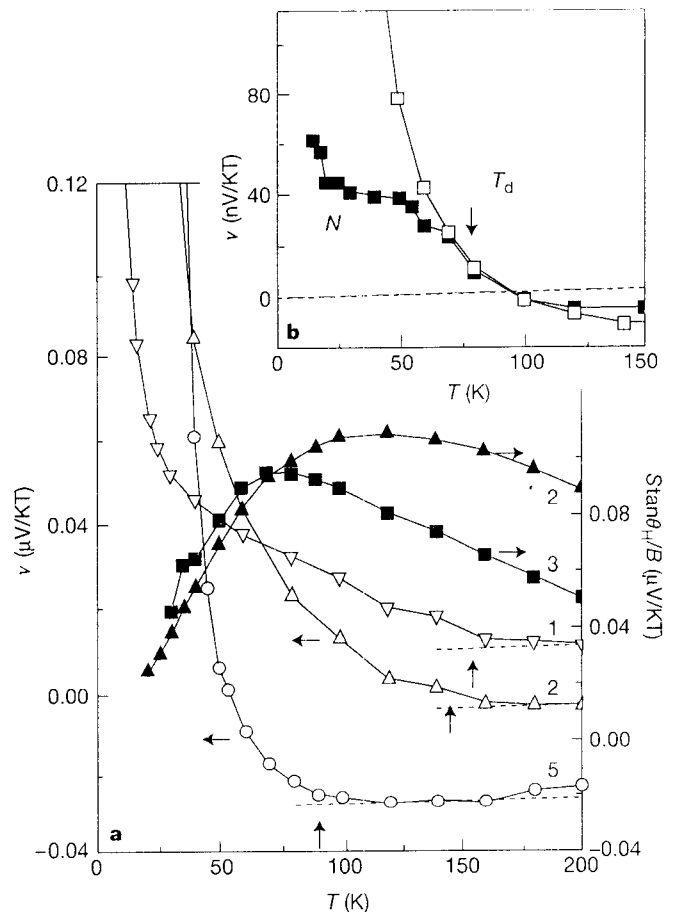


Figure 3 Nernst coefficients versus T . **a**, Expanded view of ν versus T in samples 1 (down triangles), 2 (open up triangles) and 5 (circles), showing the steep divergence of the vortex signal from the background Nernst signal (shown as broken lines). **b**, Comparison of ν in sample 3 ($x = 0.10$, open symbols) with ν in Nd-doped LSCO (sample N, with $y = 0.60$ and $x = 0.10$, solid symbols). In **a**, arrows indicate T_{onset} . The solid symbols represent the contribution $S \tan\theta_H/B$ to ν in samples 2 and 3 (see equation (2)) obtained by measuring S and $\tan\theta_H$ independently. Above T_{onset} , cancellation between the two terms in equation (2) suppresses ν to values 10–30 times smaller than $S \tan\theta_H/B$. In the absence of vortices, the experimental constraint $J_x = 0$ leads to two equal and opposite currents parallel to \mathbf{x} : that is, $\alpha(-\partial_x T) + \sigma E_x = 0$ (whence $S = \alpha/\sigma$). In finite $\mathbf{H} \parallel \mathbf{z}$, the fields $(-\partial_x T)$ and E_x generate transverse Hall currents (along y) of opposite signs. The constraint $J_y = 0$ leads to $\alpha_{yx}(-\partial_x T) + \sigma_{yx} E_x + \sigma E_y = 0$ (we neglect $-\partial_y T$, which is very small in copper oxides). Near-cancellation between the first two terms leads to a small E_y , which is observed as the Nernst signal (equation (2)). The data show that the third term is 10–30 times smaller than either of the other two. The comparison in **b** highlights the sensitivity of the divergent Nernst signal to the structural transition occurring at T_d . ν in samples 3 and N are nominally equal from 150 K to $T_d = 74$ K (arrow). Below T_d , ν remains near 40 nV/KT in sample N, whereas it increases by a further factor of 50 in sample 3.

is, the two terms in equation (2) differ by only 1 part in 30. Hence, the background Nernst signal is weakly T dependent, and about 100–500 times weaker than the peak vortex signal. The comparison shows that the possibility is very remote that the divergent Nernst signal arises from the charge carriers.

As a further test, we compare the Nernst signal in sample 3 ($x = 0.10$) with that in a Nd-doped LSCO crystal (sample N) with the same x (see Fig. 3 inset). The Nd impurities induce a structural transition at $T_d = 74$ K. Charge ordering below T_d , consistent with static stripe formation¹³, strongly suppresses the onset of the Meissner state to below 5 K. Hence, we expect superconducting fluctuations to be strongly suppressed below T_d . If the divergent component of the Nernst signal in Nd-free samples indeed originates from vortices, it should also be markedly affected below T_d . Our measurements (Fig. 3 inset) show that, from 150 K to T_d , ν in the Nd-doped crystal increases rapidly (and is very close to the value in sample 3). Below T_d , however, ν in sample N remains at the value of 40 nV/KT, whereas it grows by a further factor of 50 in sample 3. The comparison confirms that when superconducting fluctuations are strongly suppressed below T_d , there is a near-complete suppression of the divergent part of ν . This provides strong support for our identification of the divergent part of ν with a vortex-like excitation clearly related to superconducting pairing, but occurring up to 120 K above the Meissner onset at T_c .

Although we believe that the evidence for such identification is very strong, it remains to be confirmed by more direct means, such as imaging. Moreover, the finding raises the following two questions: (1) Is it confined to the LSCO family? We have nearly completed similar measurements in underdoped $\text{YBa}_2\text{Cu}_3\text{O}_y$ and Zn-doped $\text{YBa}_2(\text{Cu}_{3-x}\text{Zn}_x)\text{O}_y$ (ref. 14). Underdoped YBCO ($y = 6.40$ and 6.60) and Zn-doped YBCO show enhanced Nernst signals extending to 100–130 K, broadly similar to those reported here. The exception is over-doped YBCO ($y = 7.0$), in which the Nernst signal vanishes abruptly above about 95 K. (2) Are there other explanations for the enhanced Nernst signal? For convenience,

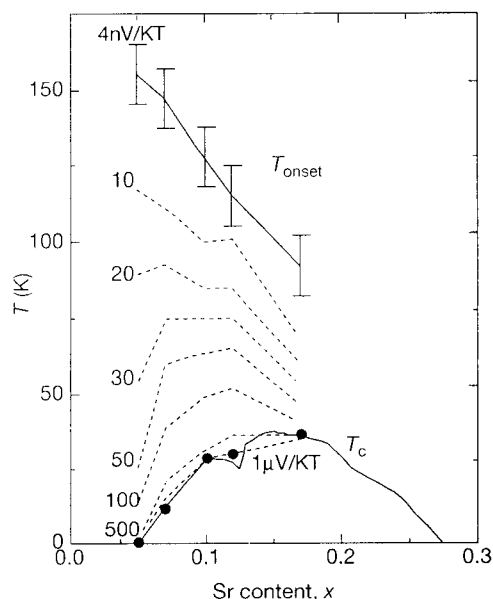


Figure 4 Contour plot of $(\nu - \nu_n)$ versus x in the phase diagram of LSCO. The contour plot displays how high in T the vortex-like excitations extend for each value of x . The upper solid line T_{onset} is the contour set by our resolution. The pseudogap T^* estimated from heat capacity¹⁵ is about a factor of two larger than T_{onset} . Values of T_c in our samples (circles) match the T_c line (lower solid line) from Takagi *et al.*¹⁴ We note that the T_c line is roughly similar to the contour line $\nu = 1 \mu\text{V/KT}$.

we divide the data into a low- T region in which ν strongly diverges towards T_c , and a high- T region where it smoothly tends asymptotically to ν_n as T increases (Fig. 3). As we argued from the data in Fig. 3b, the low- T divergence (below T_d) is suppressed in parallel with superconductivity, so it must be intimately related to Cooper pair formation. Above T_d (74 K), however, this test cannot be invoked to exclude a non-vortex origin; for example, the cancellation in equation (2) may be spoiled by dynamic stripe formation. This objection is best addressed experimentally, by doping with Zn (in YBCO, Zn is highly effective (Y. W. *et al.*, unpublished work) in removing all the anomalous signal at high T).

Finally, we cannot exclude the interesting possibility that the enhanced signal originates from an unsuspected novel excitation in the pseudogap state that binds a fluxoid, and responds to the thermal gradient. This question merits further study.

With these caveats in mind, we display as contour plots the anomalous signal $(\nu - \nu_n)$ in the phase diagram of LSCO (broken lines in Fig. 4). The plot provides an overview of how high in T the anomalous signal extends for various x . The smaller x is, the higher the signal extends, as noted above. However, the large-amplitude contours (for $1 \mu\text{V/KT}$, say) tend to follow the T_c line. We define the contour set by our resolution (4 nV/KT) as T_{onset} . These features strongly suggest that, although T_{onset} measures the highest temperature of the vortex-like excitations, the Meissner state is stable only when ν exceeds 1–2 $\mu\text{V/KT}$ (this is also evident in Fig. 2). Values of the pseudogap T^* in LSCO are less certain than in YBCO. From heat capacity measurements^{1,15}, $T^* \approx 350$ K at $x = 0.08$, and falls linearly to ~ 90 K at $x = 0.22$. With this estimate, T_{onset} is only half as large as T^* . Over the doping range investigated, T_{onset} decreases with x as the pseudogap temperature. This suggests that T_{onset} and T^* may be controlled by the same energy scale. □

Received 6 March; accepted 27 May 2000.

1. Timusk, T. & Statt, B. The pseudogap in high-temperature superconductors: an experimental survey. *Rep. Prog. Phys.* **62**, 61–122 (1999).
2. Loeser, A. G. *et al.* Excitation gap in the normal state of $\text{Bi}_2\text{Sr}_2\text{CaCu}_2\text{O}_{8+x}$. *Science* **273**, 325–329 (1996).
3. Ding, H. *et al.* Spectroscopic evidence for a pseudogap in the normal state of underdoped high- T_c superconductors. *Nature* **382**, 51–54 (1996).
4. Emery, V. J. & Kivelson, S. A. Importance of phase fluctuations in superconductors with small superfluid density. *Nature* **374**, 434–437 (1995).
5. Norman, M., Randeria, M., Ding, H. & Campuzano, J. C. Phenomenology of the low-energy spectral function in high- T_c superconductors. *Phys. Rev. B* **57**, 11093–11096 (1998).
6. Lee, P. A. & Wen, X. G. Unusual superconducting state of underdoped cuprates. *Phys. Rev. Lett.* **78**, 4111–4114 (1997).
7. Corson, J., Malozzi, R., Orenstein, J., Eckstein, J. N. & Bozovic, I. Vanishing of phase coherence in underdoped $\text{Bi}_2\text{Sr}_2\text{CaCu}_2\text{O}_{8+x}$. *Nature* **398**, 221–223 (1999).
8. Ambegaokar, V., Halperin, B. I., Nelson, D. R. & Siggia, E. D. Dynamics of superfluid films. *Phys. Rev. B* **20**, 1806–1826 (1980).
9. Hagen, S. L., Lobb, C. J., Greene, R. L., Forrester, M. G. & Talvacchio, J. Flux-flow Nernst effect in epitaxial $\text{YBa}_2\text{Cu}_3\text{O}_7$. *Phys. Rev. B* **42**, 6777–6780 (1990).
10. Ri, H. C. *et al.* Nernst, Seebeck, and Hall effect in the mixed state of $\text{YBa}_2\text{Cu}_3\text{O}_{7-x}$ and $\text{Bi}_2\text{Sr}_2\text{CaCu}_2\text{O}_{8+x}$ —a comparative study. *Phys. Rev. B* **50**, 3312–3329 (1994).
11. Clayhold, J. A., Limun, A. W. Jr, Chen, F. & Chu, C. W. Normal-state Nernst effect in a $\text{TlBa}_2\text{CaCu}_2\text{O}_{8+x}$. *Phys. Rev. B* **50**, 4252–4255 (1994).
12. Sondheimer, E. H. The theory of the galvanomagnetic and thermomagnetic effects in metals. *Proc. R. Soc. Lond. A* **193**, 484–512 (1948).
13. Tranquada, J. M., Sternlieb, B. J., Axe, J. D., Nakamura, Y. & Uchida, S. Evidence for stripe correlations of spins and holes in copper oxide superconductors. *Nature* **375**, 561–563 (1995).
14. Takagi, H., Ido, T., Ishibashi, S., Uota, M. & Uchida, S. Superconductor-to-nonsuperconductor transition in $(\text{La}_{1-x}\text{Sr}_x)_2\text{CuO}_4$ as investigated by transport and magnetic measurements. *Phys. Rev. B* **40**, 2254–2261 (1989).
15. Loram, J. W., Mirza, K. A., Cooper, J. R., Athanassopoulou, N. & Liang, W. Y. in *Proc. 10th HTS Anniversary Workshop on Physics, Materials and Applications* (eds Batlogg, B., Chu, C. W., Chu, W. K., Gubser, D. U. & Muller, K. A.) 341 (World Scientific, Singapore, 1996).

Acknowledgements

Helpful comments by P. W. Anderson, P. A. Lee and Z. Weng are acknowledged. The research is supported by the US Office of Naval Research and the US National Science Foundation. N.P.O. and S.U. acknowledge support from the New Energy and Industrial Technology Development Organization, Japan.

Correspondence and requests for materials should be addressed to N.P.O. (e-mail: npo@princeton.edu).